Studies of the Structure and Organization of Cationic Lipid Bilayer Membranes: Calorimetric, Spectroscopic, and X-Ray Diffraction Studies of Linear Saturated P-O-Ethyl Phosphatidylcholines

Ruthven N. A. H. Lewis,* Ingrid Winter,† Manfred Kriechbaum,† Karl Lohner,† and Ronald N. McElhaney*
*Department of Biochemistry, University of Alberta, Edmonton, Alberta T6G 2H7, Canada; and †Institut für Biophysik und Röntgenstrukturforschung, Österreichische Akademie der Wissenschaften, A-8042 Graz, Austria

ABSTRACT Differential scanning calorimetry, x-ray diffraction, and infrared and ^{31}P-nuclear magnetic resonance (^{31}P-NMR) spectroscopy were used to examine the thermotropic phase behavior and organization of cationic model membranes composed of the P-O-ethyl esters of a homologous series of n-saturated 1,2-diacyl phosphatidylcholines (Et-PCs). Differential scanning calorimetry studies indicate that on heating, these lipids exhibit single highly energetic and cooperative endothermic transitions whose temperatures and enthalpies are higher than those of the corresponding phosphatidylcholines (PCs). Upon cooling, these Et-PCs exhibit two exothermic transitions at temperatures slightly below the single endotherm observed upon heating. These cooling exotherms have both been assigned to transitions between the liquid-crystalline and gel phases of these lipids by x-ray diffraction. The x-ray diffraction data also show that unlike the parent PCs, the chain-melting phase transition of these Et-PCs involves a direct transformation of a chain-interdigitated gel phase to the lamellar liquid-crystalline phase for the homologous series of $n \geq 14$. Our ^{31}P-NMR spectroscopic studies indicate that the rates of phosphate headgroup reorientation in both gel and liquid-crystalline phases of these lipids are comparable to those of the corresponding PC bilayers. However, the shape of the ^{31}P-NMR spectra observed in the interdigitated gel phase indicates that phosphate headgroup reorientation is subject to constraints that are not encountered in the non-interdigitated gel phases of parent PCs. The infrared spectroscopic data indicate that the Et-PCs adopt a very compact form of hydrocarbon chain packing in the interdigitated gel phase and that the polar/apolar interfacial regions of these bilayers are less hydrated than those of corresponding PC bilayers in both the gel and liquid-crystalline phases. Our results indicate that esterification of PC phosphate headgroups results in many alterations of bilayer physical properties aside from the endowment of a positively charged surface. This fact should be considered in assessing the interactions of these compounds with naturally occurring lipids and with other biological materials.

INTRODUCTION

The phospholipids of eukaryotic cell membranes are either zwitterionic or anionic at neutral pH, and thus the lipid bilayers of such membranes possess a net negative charge. Moreover, aqueous dispersions of these phospholipids, alone or in combination with other lipids such as cholesterol, can form closed vesicles or liposomes, and these have been widely used to deliver drugs to cells and organisms (see Gregoriadis, 1995). Nevertheless, lipid-like molecules bearing a positive charge can also form liposomes and, alone or in combination with natural phospholipids, these cationic amphiphiles have also proven useful in various medical, technical, and cosmetic applications (see Konstantinova and Serebrinnikova, 1996). However, the most important application of cationic amphiphiles is probably their ability to deliver DNA to eukaryotic cells (see Morgan and Anderson, 1993; Felger, 1995). Moreover, cationic amphiphiles have recently also been used to deliver antisense oligonucleotides and proteins to such cells (Debs et al., 1990; Zhou and Huang, 1994; Huang et al., 1995; Barber et al., 1996; Bennett et al., 1992).

The compounds utilized to date to deliver DNA and other materials to cells are usually described in the literature as "cationic lipids," although in fact they are mostly cationic amphiphiles or detergents that are not closely related chemically to naturally occurring phospholipids. Moreover, because of their different chemical structures, in particular the absence of ester bonds in the polar headgroup region, these cationic amphiphiles are at best only partially metabolizable and may thus accumulate and exhibit toxicity in whole animal or human applications. For these and other reasons it would be desirable to develop cationic lipids that more closely resemble naturally occurring phospholipids both chemically and physically.

Cationic triesters of phosphatidylcholine (P-O-ethyl phosphatidylcholine; Et-PC), prepared from phosphatidylcholines (PCs) through substitution of an alkyl group on the phosphate oxygen of the polar headgroup, appear to be promising candidates for DNA transfection and other scientific and biomedical applications (Gorman et al., 1997; McDonald et al., 1998; MacDonald et al., 1999a, b; Matsumura et al., 1999). These compounds are chemically stable, hydrate well, and disperse readily in water to form closed liposomes, and such vesicles readily fuse with erythrocytes and anionic lipid vesicles (Pantazatos and MacDonald,

Received for publication 18 April 2000 and in final form 1 December 2000.
Address reprint requests to Ronald N. McElhaney, Department of Biochemistry, University of Alberta, Edmonton, Alberta T6G 2H7, Canada. Tel.: 780-492-2413; Fax: 780-492-0095; E-mail: rmcelhan@gpu.srv.ualberta.ca.

0006-3495/01/03/1329/14 $2.00

1999; MacDonald et al., 1999a, b). Cationic triesters of PC also form complexes with DNA and exhibit great effectiveness as transfective agents, but are well metabolized and exhibit a low toxicity in cell cultures (McDonald et al., 1998; MacDonald et al., 1999b). Moreover, these cationic PC analogs exhibit gel/liquid-crystalline phase transitions at temperatures close to those exhibited by the corresponding PCs, although they are more surface-active and exhibit a higher surface potential than their parent compounds (MacDonald et al., 1999a). These and other differences in their physical behavior were ascribed to their net positive charge and to the absence of intermolecular hydrogen bonding between adjacent polar headgroups in the lipid bilayer (MacDonald et al., 1999a, b). Finally, we have recently shown that cationic triesters of PC are very useful compounds for studies of the effect of variations of surface charge density on the interactions of the antimicrobial peptide gramicidin S with lipid bilayers (Lewis et al., 1999) and on phospholipid lamellar/nonlamellar phase preferences (Lewis and McElhaney, 2000).

We present here the results of a study of the thermotropic phase behavior, structure, and organization of aqueous dispersions of a series of linear saturated P-O-ethyl esters of phosphatidylcholine utilizing the techniques of DSC, x-ray diffraction, and ^{31}P-NMR and FTIR spectroscopy. The goal of these studies is to provide the basic physical information required for the fullest scientific, technical, and biomedical exploitation of these promising cationic phospholipids. Our findings indicate that many of the physical properties of bilayers of these compounds are appreciably different from those of the parent compounds, most notably in their ability to form interdigitated bilayers in the gel state. Interestingly, not all of these differences are easily rationalized on the basis of the charge or hydrogen bonding potential of the cationic triester polar headgroup.

MATERIALS AND METHODS

Lipids

The P-O-ethyl esters of dilauroyl, dimyristoyl, dipalmitoyl, and distearoyl PC (Et-DLPC, Et-DMPC, Et-DPPC, and Et-DSPC, respectively) were purchased from Avanti Polar Lipids Inc. (Alabaster, AL) and were used without further purification. Sample purity was checked by thin-layer chromatography using the solvent system, $CHCl_3/CH_3OH/NH_{3,conc}$ (65:25:4 by volume). At the completion of the biophysical measurements described below, the Et-PCs were checked for possible chemical degradation using the above methodology, but no such degradation could be detected.

Differential scanning calorimetry

Samples were prepared for DSC by dispersing 3–5 mg of the dried lipid in 0.5 ml buffer containing 50 mm Tris, 100 mM NaCl, 1 mM EDTA, 1 mN NaN_3 pH 7.4 at temperatures some 20°C above the gel/liquid-crystalline phase transition temperature (T_m) of the hydrated lipid by intermittent Vortex mixing. The dispersions so obtained were examined in a high-sensitivity multi-cell Hart differential scanning calorimeter (Calorimetry Sciences Corporation, Provo, UT) at scan rates of 10°C/h. Heating and cooling thermograms were recorded at temperatures between −7°C and 20°C above the main phase transition of the lipid.

^{31}P-NMR spectroscopy

For the ^{31}P-NMR spectroscopic experiments, samples were prepared by dispersing 10–15 mg of the dried lipid in 0.6 ml of the same buffer used for the DSC measurements. Samples were dispersed by vigorous agitation at temperatures some 20°C above the T_m of the lipid concerned, and the dispersions were subsequently heated and cooled between fluid phase temperatures and −20°C three times before initial data acquisition. Spectra were recorded with a Varian Unity 300 Fourier Transform spectrometer (Varian Inc., Palo Alto, CA) operating at 121.41 MHz for ^{31}P using single-pulse data acquisition techniques and other data acquisition parameters similar to those described by Lewis et al. (1988). The data were analyzed using computer software supplied by the instrument manufacturers and were plotted with the Origin software package.

X-ray diffraction

Samples for the x-ray experiments were prepared by dispersing 8 mg of the lipid sample in 100 μl sodium phosphate buffer (100 mM phosphate, 1 mM NaN_3, pH 7.4) at ~60°C by intermittent Vortex mixing. X-ray diffraction experiments were performed on a SWAX-camera (HECUS M. Braun, Graz, Austria), which allows simultaneous recording of diffraction data in both the small- and wide-angle regions. Nickel-filtered CuK_α-radiation ($\lambda = 0.154$ nm), originating from a Philips x-ray generator with a copper anode operating at 50 kV and 40 mA, was used. The camera was equipped with a Peltier-controlled variable-temperature cuvette and a one-dimensional position-sensitive detector OED 50-M (M. Braun, Garching, Germany). Calibration in the small-angle region was performed with silver stearate and in the wide-angle region with a *p*-bromo-benzoic acid standard, respectively. Temperature control was achieved by a programmable temperature control system (MTC-2.0, HECUS M. Braun, Graz, Austria) which enabled temperature control between 1°C and 65°C with a precision of ±0.1°C. Samples were loaded into quartz capillaries that were thermally equilibrated for 10 min before initiating data acquisition using the program ASA V2.3 (HECUS M. Braun, Graz, Austria). Multiplexed exposure times of 1800 s for both the small-angle and wide-angle region were chosen.

Small-angle x-ray diffraction data arising from particle scattering were further analyzed by indirect Fourier transformation. In the case of flat particles such as extended lamellar structures, where the axial thickness of the lamella is much smaller than its surface area, the one-dimensional distance distribution function $p_t(r)$ can be derived from the scattering data. This represents the autocorrelation function of the electron density normal to the bilayer plane, which yields information on the cross-bilayer distance between the electron-dense phosphate groups ($d_{P\text{-}P}$), i.e., the phosphate groups located in the opposing monolayers of the bilayer, and on the bilayer thickness (d_m). Thereby, $d_{P\text{-}P}$ can be determined from the position of the outer maximum of the $p_t(r)$-function and d_m from the point where the $p_t(r)$-function approaches zero. Briefly, $p_t(r)$ were computed after background subtraction and normalization of the respective buffer blank curve and data-point reduction of the difference curve by a funneling routine. Furthermore, the data were corrected for instrumental broadening by using the program ITP (Glatter, 1977) to yield desmeared data, which were interpreted in real space in terms of their pair distance distribution function (Glatter, 1982a, b).

Electron density ($\rho(r_z)$) profiles normal to the bilayer plane were calculated for multilamellar vesicles in the gel phase using the standard procedure described by Wiener et al. (1989). After subtraction of the background, the Lorentz-corrected Bragg peaks were integrated and the square root of the peak area was then used as the constant form factor F of

the respective peak. The electron density profile relative to the constant electron density of the buffer was calculated by the Fourier synthesis:

$$\rho(r_z) = \sum_{h=1}^{hmax} F_h \cos\left(\frac{2\pi h r_z}{d}\right)$$

where h is the order of reflection and d is the lamellar repeat distance.

FTIR spectroscopy

For the FTIR spectroscopic experiments, samples were prepared by dispersing 1–2 mg of the lipid sample in 50 μl of a D_2O-based sodium phosphate buffer (100 mM phosphate, 1 mM NaN_3, pH 7.4) at temperatures near 60°C. The mixture obtained was squeezed between the CaF_2 windows of a heatable, demountable liquid cell (NSG Precision Cells, Farmingdale, NY) equipped with a 25 μM Teflon spacer. Once mounted in the sample holder of the spectrometer, the sample temperature could be varied between −20°C and 90°C by an external, computer-controlled water bath. Infrared spectra were acquired as a function of temperature with a Digilab FTS-40 Fourier-transform spectrometer (Biorad, Digilab Division, Cambridge, MA) using data acquisition parameters similar to those described by Mantsch et al. (1985). The experiment involved a sequential series of 2°C temperature ramps with a 20-min inter-ramp delay for thermal equilibration, and was equivalent to a scanning rate of 4°C/h. The data obtained were analyzed using computer programs obtained from the instrument manufacturer and from the National Research Council of Canada, and plotted with the Origin software package. In cases where absorption bands appeared to be a summation of components, a combination of Fourier deconvolution and curve-fitting procedures was used to obtain estimates of the position of the component bands and to reconstruct the contours of the original band envelope.

RESULTS

Differential scanning calorimetry

Presented in Fig. 1 are DSC heating and cooling thermograms illustrating the thermotropic phase behavior exhibited by aqueous dispersions of the four Et-PCs studied here. The pattern of phase behavior illustrated therein remained unchanged after extensive incubation at low temperatures. These compounds all exhibit a single, highly cooperative, highly energetic endothermic phase transition on heating, which has been assigned to an interdigitated gel ($L_{\beta I}$) to lamellar liquid-crystalline (L_α) phase transition by our spectroscopic and x-ray diffraction data (see below). These endothermic phase transitions occur at temperatures slightly above those of the gel/liquid-crystalline phase transitions of the corresponding unesterified PCs, and the transition enthalpy changes are somewhat greater than observed with the latter compounds (see Table 1). The molecular basis for these differences in phase behavior, which were also observed by MacDonald et al. (1999a), will be discussed below. Upon cooling, aqueous dispersions of these compounds exhibit two exothermic events. Of these, the higher

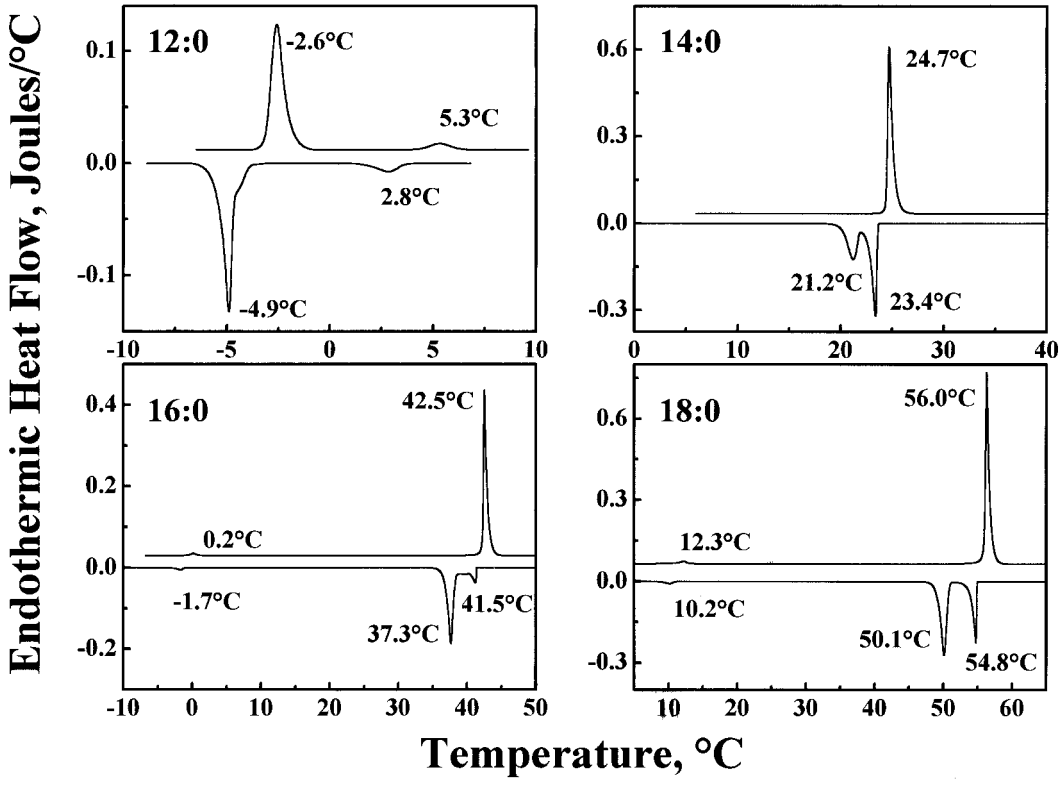

FIGURE 1 DSC thermograms exhibited by aqueous dispersions of the four linear saturated P-O-ethyl PCs studied. The thermograms shown were acquired at heating rates near 10°C/h in a buffer containing 50 mM Tris, 100 mM NaCl, 1 mM EDTA, 1 mM NaN_3, pH 7.4.

Table 1. Thermodynamic characterization of the thermotropic phase transitions exhibited by the *P-O*-ethyl esters of the *N*-saturated 1,2-diacylphosphatidylcholines

Chain Length *N**	Transition Temperature (°C)	Transition Type	Enthalpy Change (kcal/mol)
12:0	−2.6	L_{β}[†]/L_{α}	4.3
12:0	5.3	L_{α}/L_{α}	0.5
14:0	≅22[‡]	$L_{\beta I,o}$[§]/$L_{\beta I,h}$	unknown
14:0	24.7	$L_{\beta I,h}/L_{\alpha}$	7.6
16:0	0.2	$L_{\beta I,o}$[§]/$L_{\beta I,h}$	0.4
16:0	42.5	$L_{\beta I,h}/L_{\alpha}$	9.6
18:0	12.3	$L_{\beta I,o}/L_{\beta I,h}$	0.4
18:0	56.0	$L_{\beta I,h}/L_{\alpha}$	12.3

All values estimated from heating mode experiments.
*Number of carbon atoms per acyl chain.
[†]The nature of this lamellar gel phase is unknown. The T_m of this lipid is below the temperature range accessible to the x-ray diffraction experiment used.
[‡]Estimated from analogous temperature-dependent changes in the FTIR spectra (see text).
[§]The interdigitated gel phase with orthorhombic hydrocarbon chain packing was not determined by x-ray diffraction owing to its appearance below 0°C, but can be proposed to be analogous to that of Et-DSPC. $L_{\beta I,o}$, interdigitated lamellar gel with orthorhombic hydrocarbon chain packing; $L_{\beta I,h}$, interdigitated lamellar gel with hexagonal chain packing.

temperature exotherm is observed at temperatures slightly below the chain-melting phase transition observed upon heating and the lower-temperature exotherm is observed some 2–4°C lower. Also, the temperature resolution of these exothermic events increases as hydrocarbon chain length increases. Moreover, the combined enthalpy of the two thermotropic events observed upon cooling is comparable to that of the single endothermic event observed upon heating. Fig. 1 also shows that the longer-chain Et-PCs exhibit a reversible, weakly energetic (~0.3–0.5 kcal/mol) thermotropic event at temperatures some 40°C below the $L_{\beta I}/L_{\alpha}$ phase transition alluded to above. Our spectroscopic and x-ray diffraction data suggest that this is a gel-gel phase transition in which the packing arrangement of the lipid hydrocarbon chains change (see below). Finally, Fig. 1 also shows that aqueous dispersions of the dilauroyl derivative exhibit an unidentified reversible thermotropic event that is weakly energetic (~0.3 kcal/mol) and occurs at temperatures some 8°C above its hydrocarbon chain-melting phase transition. Our spectroscopic and x-ray diffraction studies suggest that this process is not a lamellar/nonlamellar phase transition (see below). The physical basis of this and the other thermotropic events exhibited by these compounds were examined in greater detail in the x-ray diffraction and spectroscopic studies described below.

^{31}P-NMR spectroscopy

^{31}P-NMR spectra of the various Et-PCs were acquired over temperature ranges that bracket all of the thermotropic events resolved in our DSC studies. The data shown in Fig. 2 were acquired with Et-DPPC, but all of the Et-PC dispersions studied behave similarly. A comparable set of ^{31}P-NMR spectra acquired with the corresponding unesterified derivative (DPPC) is presented in Fig. 3 as a reference. At temperatures well below the onset of the main phase transition (i.e., $T_m - T \geq 5$°C), the Et-PCs exhibit powder patterns that are relatively broad (basal linewidths ≅ 100 ppm) and centered near 0 ppm. Upon heating from low temperatures, the overall shape and widths of these spectra

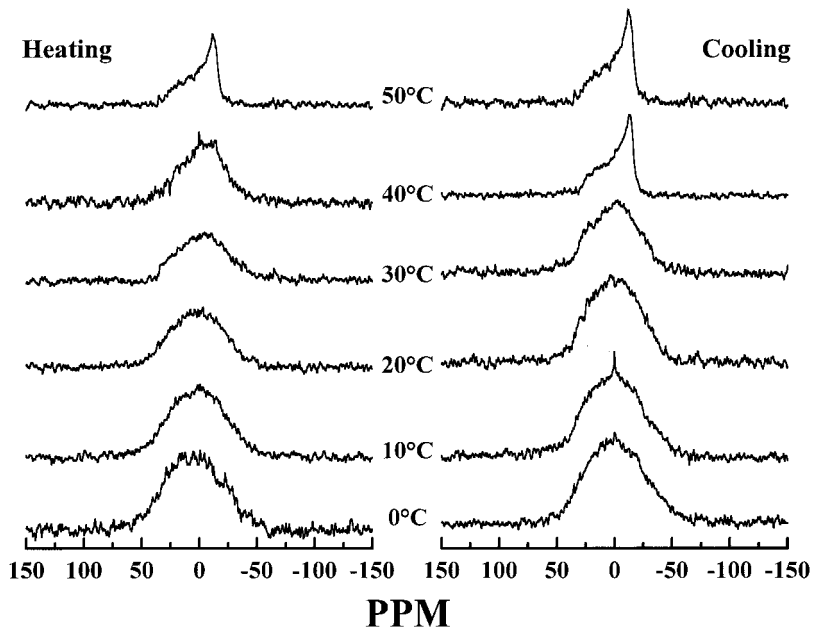

FIGURE 2 Proton-decoupled ^{31}P-NMR powder patterns exhibited by aqueous dispersions of Et-DPPC. The spectra displayed were acquired at the temperatures indicated in both heating (*left panel*) and cooling (*right panel*) modes.

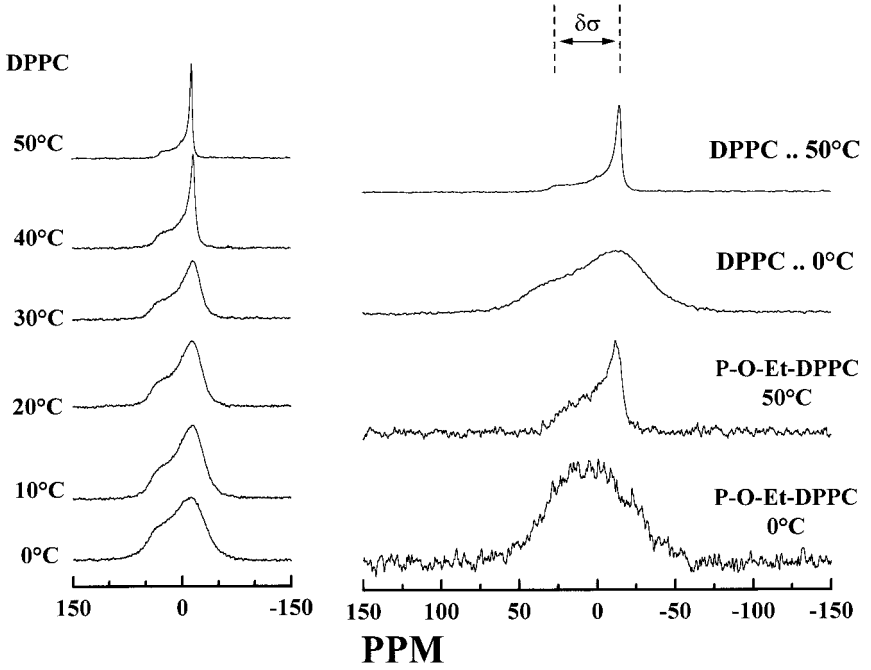

FIGURE 3 A comparison of the ^{31}P-NMR powder patterns exhibited by aqueous dispersions of DPPC and Et-DPPC. The left panel shows representative temperature-dependent changes in the ^{31}P-NMR spectra of aqueous DPPC between 0 and 50°C. The right panel shows a comparison of the ^{31}P-NMR spectra of DPPC and Et-DPPC in the gel (0°C) and liquid-crystalline (50°C) state. $\delta\sigma$ indicates the chemical shielding anisotropy estimated from the DPPC spectra.

do not change significantly until the temperature approaches the onset of the hydrocarbon chain-melting phase transition. At higher temperatures, the broad features collapse and the powder pattern adopts a lineshape characteristic of randomly oriented phospholipid bilayers in which there is fast axially symmetric motion of the phosphate headgroup about the axis of reorientation, the bilayer normal (see Seelig, 1978; Campbell et al., 1979). Moreover, aside from slight thermally induced decreases in overall linewidth, further heating of the samples does not result in significant changes in the shape of the spectra observed. These observations indicate that these Et-PCs form only lamellar phases at all temperatures above the T_m. Thus, the weakly energetic thermotropic event exhibited by Et-DLPC about 8°C above the gel/liquid-crystalline phase transition does not involve a lamellar/nonlamellar phase conversion, or indeed any major change or structural reorganization of the lipid bilayer. It should also be noted that the weakly energetic transition observed by calorimetry at temperatures some 40°C below the main phase transition of the longer chain compounds is also not accompanied by any discernible changes in the ^{31}P-NMR spectra. Evidently this weak solid phase transition does not significantly alter the motion and reorientation of the phosphate headgroup. Finally, with all of the compounds studied, the spectroscopic changes alluded to above are fully reversed upon cooling, albeit with some hysteresis comparable to that observed in the DSC experiment (see Fig. 2).

A comparison of the temperature-dependent changes in the ^{31}P-NMR spectra of these Et-PCs derivatives with those normally exhibited by unesterified PCs such as DPPC reveals other interesting and structurally relevant features. As illustrated in Fig. 3, the L_α phases of common phospholipids such as DPPC exhibit ^{31}P-NMR powder patterns consistent with fast axially symmetric motion of the phosphate headgroup about the bilayer normal. For such spectra, the residual chemical shielding anisotropy values ($\delta\sigma$, see Fig. 3) are usually ~40 ppm. Interestingly, similar values are noted for the Et-PC studied here, suggesting that in the L_α phase the range and amplitudes of reorientational motions of the phosphate moieties of bilayers composed of both types of PCs are comparable. However, Fig. 3 also shows that upon cooling to temperatures below the T_m, the ^{31}P-NMR spectra of phospholipids such as DPPC exhibit a discontinuous increase in the overall spectral linewidth at the gel/liquid-crystalline phase transition temperature, followed by smaller but continuous increases in linewidth as the temperature decreases. However, the general features of the powder pattern and its chemical shielding anisotropy are essentially similar to those observed in the L_α phase. Thus, despite significant decreases in the rates of phosphate reorientation upon conversion to the gel phase, phosphate motions continue to be axially symmetric about the bilayer normal. These observations contrast sharply to the behavior observed in the $L_{\beta I}$ phases of the P-O-ethyl derivatives examined here. As illustrated in Figs. 2 and 3, the general shape of the powder patterns exhibited by the Et-PCs change significantly upon conversion to the $L_{\beta I}$ phase and do not exhibit the features normally associated with axially symmetric motion about the bilayer normal. Moreover, the spectral linewidths observed in the gel phases of Et-DPPC are less sensitive to temperature changes than are those of lipids such as DPPC. However, the basal line widths of the observed gel phase powder patterns are comparable in both

Et-DPPC and DPPC at temperatures near 0°C, suggesting that the overall rates of phosphate reorientation occurring in the gel phases of both lipids are comparable. The possible molecular basis of these ^{31}P-NMR spectroscopic observations will be explored below and in the Discussion.

X-ray diffraction

Small- and wide-angle x-ray scattering profiles of fully hydrated dispersions of the Et-PCs were acquired at temperatures bracketing the phase transitions of these lipids observed calorimetrically. With Et-DLPC, all x-ray measurements were performed in the L_α phase because the T_m of this lipid is below the temperature range of our instrument. At all temperatures examined this lipid exhibits broad diffuse wide-angle reflections that are characteristic of melted hydrocarbon chains (Tardieu et al., 1973). In the small-angle region, Et-DLPC exhibits continuous x-ray scattering curves characteristic of single, uncorrelated bilayers (Bouwstra et al., 1993; Laggner, 1994). This enabled the use of indirect Fourier transformation methods (see Glatter, 1982a, b) to calculate one-dimensional distance distribution functions $p_t(r)$, which encode information on the d_m and on the $d_{P\text{-}P}$ between the electron-dense phosphate groups located in the opposing monolayers of the bilayer. An examination of the one-dimensional distance distribution functions at temperatures bracketing the higher-temperature transition exhibited by Et-DLPC indicates that the d_m (~39 Å) does not change upon progression through the weak thermotropic phase transition centered near 5°C. However, a small but significant decrease (≅1 Å) in $d_{P\text{-}P}$ occurs at this temperature (see Fig. 4), suggesting that this minor transition may be the result of a cooperative change in the conformation of the polar headgroup of this lipid.

Unlike Et-DLPC, the small-angle x-ray diffraction patterns exhibited by Et-DMPC, Et-DPPC, and Et-DSPC are characterized by sharp Bragg reflections with spacing ratios of 1:2:3, which reflect a one-dimensional lattice and can be related to the lamellar repeat periodicity of multilamellar structures (see Hui et al., 1984; Kriechbaum and Laggner, 1996). The small-angle x-ray diffractograms shown in Fig. 5 were acquired with Et-DSPC and typify the thermotropic phenomena exhibited by the other Et-PCs examined. At temperatures well below the T_m, the diffraction patterns exhibited by these Et-PCs all show up to three orders of Bragg reflections, consistent with the existence of lamellar lattices with the d spacing values between 50 Å and 54 Å (see Table 2). Upon heating, the lamellar d spacing values of each lipid increase abruptly by some 12–14 Å at temperatures coincident with the T_m of the lipid concerned (see Fig. 6 and Table 2). An increase in lamellar d spacing at the hydrocarbon chain-melting phase transition is atypical of the behavior of most hydrated lipid bilayers, which usually exhibit a decrease in d spacing when heated through the gel/liquid-crystalline phase transition, particularly when a lipid exhibits a L_β/L_α phase transition. However, such behavior has been observed at the gel/liquid-crystalline phase transitions of lipids that form hydrocarbon-chain interdigitated gel phases (e.g., Braganza and Worcester, 1986; Laggner et al., 1987). The possibility that these cationic PC derivatives may also be forming hydrocarbon-chain interdigitated gel phases was examined by calculating the one-dimensional electron density normal to the bilayer plane.

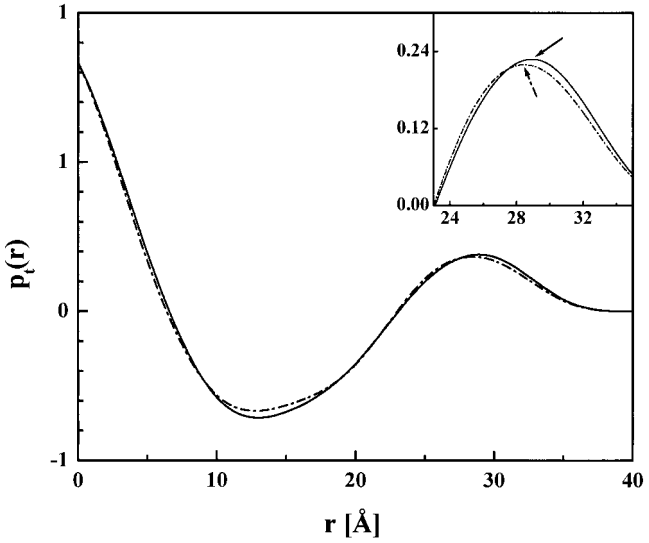

FIGURE 4 Computed one-dimensional distance distribution function $p_t(r)$ of the Et-DLPC at 1°C (*solid line*) and at 10°C (*broken line*). The arrows indicate the positions of the outer maxima, which correspond to the cross-bilayer distance between the electron-dense phosphate groups (for details see Materials and Methods).

For a centrosymmetric electron density profile such as occurs with a lipid bilayer, the phase information for each diffraction order is either +1 or −1. The only combination of phases that gave a profile consistent with a phospholipid bilayer structure is (− − +), in agreement with the observations of numerous x-ray diffraction studies of gel phase DPPC (e.g., see Wiener et al., 1989) and of chain-interdigitated lipid gel phases (for examples, see Furuike et al., 1999; Nambi et al., 1988; Hirsh et al., 1998; Huang and McIntosh, 1997). Fig. 7 shows the one-dimensional electron density profile calculated for aqueous Et-DSPC dispersions at temperatures below the T_m (35°C), whereby the origin is located at the center of symmetry of the bilayer normal. The high density peaks, located at ±18 Å, correspond to the location of the phosphates of the lipid polar headgroup, while the low density region in the center of the profile reflects the hydrocarbon chains. In contrast to electron density profiles of bilayers with noninterdigitated hydrocarbon chains, we do not observe a well-defined trough at the bilayer center, which would be characteristic for the opposing terminal methyl groups in a bilayer with noninterdigitated acyl chains. Similar observations were first reported in studies of the hydrocarbon chain-interdigitated low-temper-

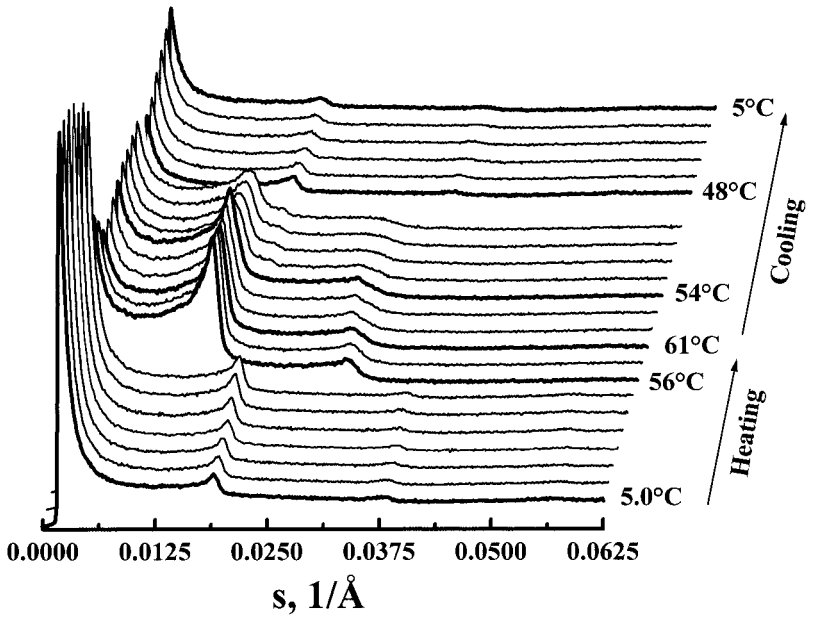

FIGURE 5 Small-angle x-ray diffractograms of fully hydrated dispersions of the Et-DSPC obtained from heating and cooling experiments, where $s = h/(2\pi)$ and $h = 4(\pi/\lambda)\sin(\Theta)$, λ being the wavelength of the x-ray beam and 2Θ the scattering angle. The data shown were acquired at the temperatures indicated.

ature phases of DPPG, where the loss of an electron density trough was correlated with the formation of a structure in which the average surface area available to each DPPG molecule is approximately four times the area of the unit cell of the hydrocarbon chain lattice, as is consistent with the formation of a fully hydrocarbon chain-interdigitated DPPG bilayer (Ranck et al., 1977). The similarity of electron density profiles described in these studies and the short distance between the headgroups across the bilayer (36 Å as compared to 54 Å that would be expected for two fully extended, untilted DSPC chains) can thus be accommodated within the context of a fully interdigitated bilayer (see Fig. 7), as has been described earlier for interdigitated hydrocarbon chain packing (e.g., Ranck et al., 1977; McIntosh et al., 1983; Kim et al., 1987). Comparable evidence supporting the formation of chain-interdigitated gel phases was also obtained in our studies of the dimyristoyl and dipalmitoyl derivatives.

Fig. 6 also shows that upon cooling Et-DSPC from temperatures near 61°C, slight temperature-dependent increases in the lattice spacing occur such that the *d* spacings approach values of 71 Å at temperatures near 53°C. With further cooling to temperatures just below 53°C, additional reflections consistent with a coexisting lamellar lattice with a *d* spacing of some 56–57 Å also appear and both reflections coexist down to temperatures near 50°C (see Figs. 5 and 6). Moreover, with the appearance of the latter reflections, a concomitant appearance of a symmetrically shaped, wide-angle Bragg reflection centered near 4.17 Å occurs (data not shown), confirming that a significant fraction of lipids (presumably those that give rise to the 56–57 Å *d* spacing) is in a lamellar gel phase with untilted hydrocarbon side chains (see below). Upon cooling, the intensity of the peak attributed to the smaller lamellar lattice grows at the expense of that emanating from the larger lamellar lattice, which disappears completely upon cooling to temperatures below 48°C. The remaining smaller lamellar lattice spacing decreases to values near 55 Å when the sample is cooled to temperatures well below the T_m. We also note that the coexistence of the two lamellar repeat spacings occurs over the same temperature range wherein two cooling exothermic transitions are resolved by DSC (Fig. 6). We therefore conclude that these two calorimetrically resolved exothermic events both involve a conversion from lamellar liquid-crystalline to comparable lamellar gel phases. The possible basis of this observation will be explored in the Discussion.

Table. 2 *d*-Spacing of the lamellar phases formed by aqueous dispersions of the *P-O*-ethyl esters of the *N*-saturated 1,2-diacylphosphatidylcholines

	d-Spacing (Å)*	
Lipid	Gel Phase (T_m − 5°C)	Liquid-Crystalline Phase (T_m)
Et-DMPC	50	62
Et-DPPC	52	64
Et-DSPC	54	68

*All values estimated from heating mode experiments.

Illustrated in Fig. 8 are the wide-angle x-ray diffraction patterns exhibited by Et-DSPC in the temperature range from 5 to 40°C. The observed diffraction peaks arise from the stacked hydrocarbon chains and can therefore provide valuable information on hydrocarbon chain packing interactions in these phospholipid bilayers. At temperatures below the calorimetrically resolved weakly energetic solid phase transition, two wide-angle diffraction peaks are observed near 4.2 Å and 3.8 Å (T = 5°C). These reflections

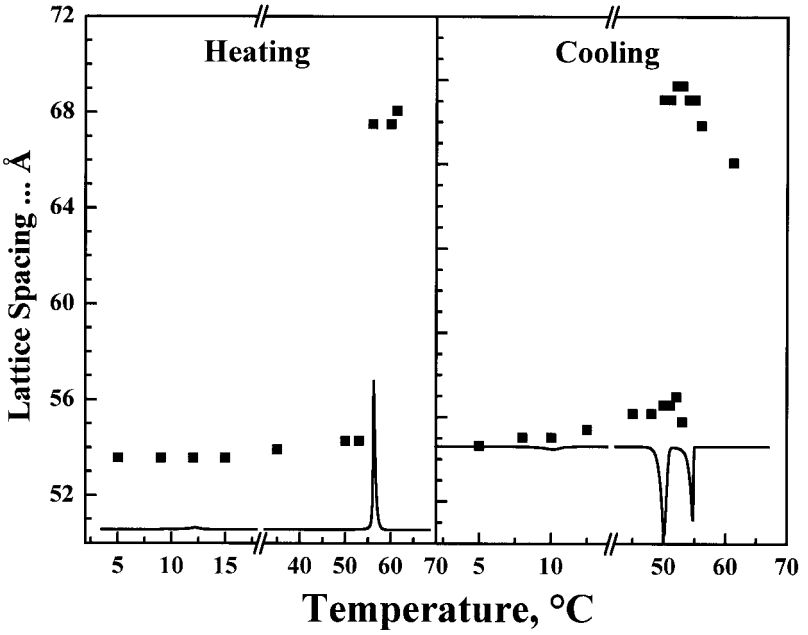

FIGURE 6 Temperature dependence of the lattice spacing exhibited by the Et-DSPC as observed upon heating (*left panel*) and cooling (*right panel*). The corresponding DSC thermograms are also shown to facilitate comparison between the two sets of data.

can be assigned to the *110* and *200* spacings of an orthorhombic subcell with lattice parameters $a = 7.60$ Å and $b = 5.04$ Å (Laggner et al., 1987; Maulik et al., 1990), and under these conditions the average area per chain is ~19.15 Å^2. Upon heating to temperatures near 10°C the position of the *110* reflection does not change, whereas the *200* reflection moves progressively to smaller scattering angles while becoming progressively broader as the temperature rises (see Fig. 8). At temperatures between 12 and 14°C (i.e., the temperature range of the solid-solid phase transition), only a single broad reflection near 4.12 Å can be resolved and this becomes progressively sharper as the temperature increases (see Fig. 8). Concomitantly, the peak position pro-

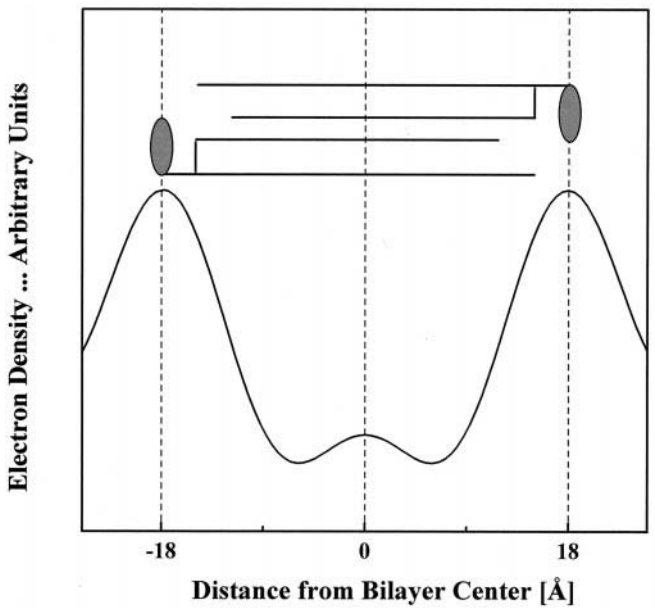

FIGURE 7 One-dimensional electron density profile along the bilayer normal calculated from the small-angle x-ray diffraction patterns of the gel phase of Et-DSPC at 35°C. The lamellar repeat distance for the sample was 54°C, the phases were (− − +) (for details see text), and the amplitudes were derived from the diffractogram as described in the Materials and Methods. A scheme illustrating the arrangement of the lipid molecules is superimposed.

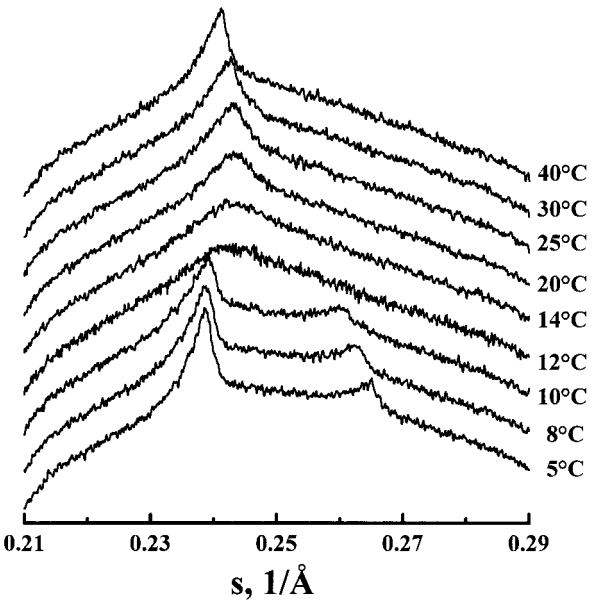

FIGURE 8 Wide-angle x-ray diffractograms of fully hydrated dispersions of the Et-DSPC; $s = h/(2\pi)$ and $h = 4(\pi/\lambda)\sin(\Theta)$, where λ is the wavelength of the x-ray beam and 2Θ the scattering angle. The data were recorded between 5 and 40°C.

gressively shifts toward values near 4.2 Å, the theoretical *010* reflection for a hexagonal subcell (Maulik et al., 1990). At these higher temperatures the lattice constants approach values of $a = b = 4.85$ Å, and the area per chain increases to values near 20.37 Å^2. The remaining single wide-angle diffraction peak persists until the onset of the hydrocarbon chain-melting phase transition, at which point the peak disappears and is replaced by a barely detectable diffuse reflection around 4.6 Å. The latter is consistent with the formation of lipid L_α phases (Tardieu et al., 1973). We therefore conclude that the weakly energetic thermotropic transition exhibited by the longer-chain compounds involves a reversible interconversion between a lower-temperature state containing orthorhombically packed all-*trans* hydrocarbon chains and a higher-temperature state with hexagonally packed all-*trans* hydrocarbon chains. This conclusion is compatible with those drawn from the results of our FTIR spectroscopic studies (see below).

FTIR spectroscopy

Illustrated in Fig. 9 are the CH_2 stretching, CH_2 bending, and C═O stretching regions of the FTIR spectra of Et-DSPC at temperatures that bracket the thermotropic transitions resolved by DSC. The spectroscopic features shown therein are typical of our FTIR spectroscopic observations of all of the Et-PCs examined. At all temperatures below the T_m, absorption bands in the CH_2 region of the spectrum are fairly sharp, consistent with the low degree of hydrocarbon chain mobility expected under such conditions. Also, the peak frequencies of the CH_2 stretching bands near 2850 cm^{-1} and 2918 cm^{-1} are essentially insensitive to temperature changes at all temperatures up to the onset of the main calorimetric phase transition. However, at the main phase transition, the symmetric and asymmetric stretching bands broaden significantly and their peak frequencies increase by 2–3 cm^{-1} and 5–7 cm^{-1}, respectively. Given that these spectroscopic changes are indicative of increased hydrocarbon chain mobility and conformational disorder (see Lewis and McElhaney, 1996, and references cited therein), our observations indicate that the main phase transition observed by DSC involves hydrocarbon chain melting. Moreover, given the results of the ^{31}P-NMR and x-ray diffraction studies presented above, we can confidently assign this thermotropic event to a $L_{\beta I}/L_\alpha$ phase transition. Given this, the weakly energetic phase transition observed at low temperature must be a solid phase event that does not involve significant changes in the mobility and conformational ordering of the lipid hydrocarbon chains.

In contrast to the C—H stretching absorption bands, the C—H bending bands of the infrared spectra of these Et-PCs show distinct changes, which coincide with the weakly energetic solid phase transition observed by calorimetry. As illustrated in Fig. 10 (*right panel*), the main CH_2 scissoring band near 1468 cm^{-1} is strongly split into components centered near 1464 cm^{-1} and 1473 cm^{-1} when samples of these lipids are cooled to very low temperatures (i.e., >40°C below T_m). This particular spectroscopic phenomenon is the so-called factor group splitting (also known as the crystal field splitting or correlation field splitting), which

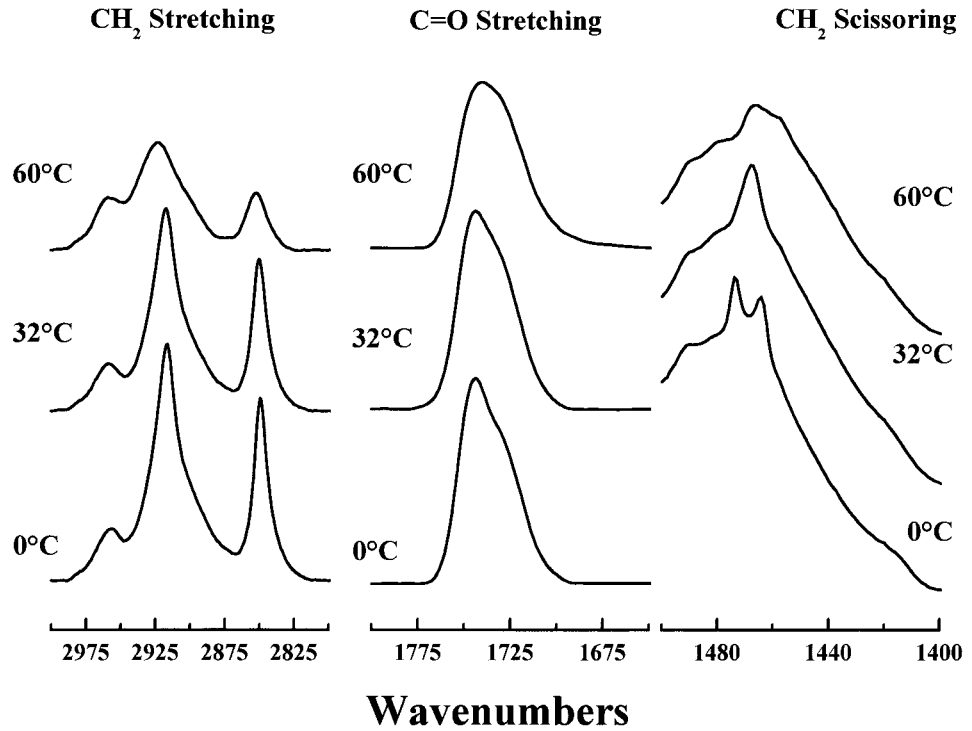

FIGURE 9 FTIR absorbance spectra showing the contours of the C—H stretching (*left panel*), C═O stretching (*middle panel*), and C—H bending (*right panel*) regions of Et-DSPC. The spectra shown were acquired at the temperatures indicated and exemplify the spectra exhibited by these compounds at temperatures bracketing the phase transitions observed in the DSC experiment.

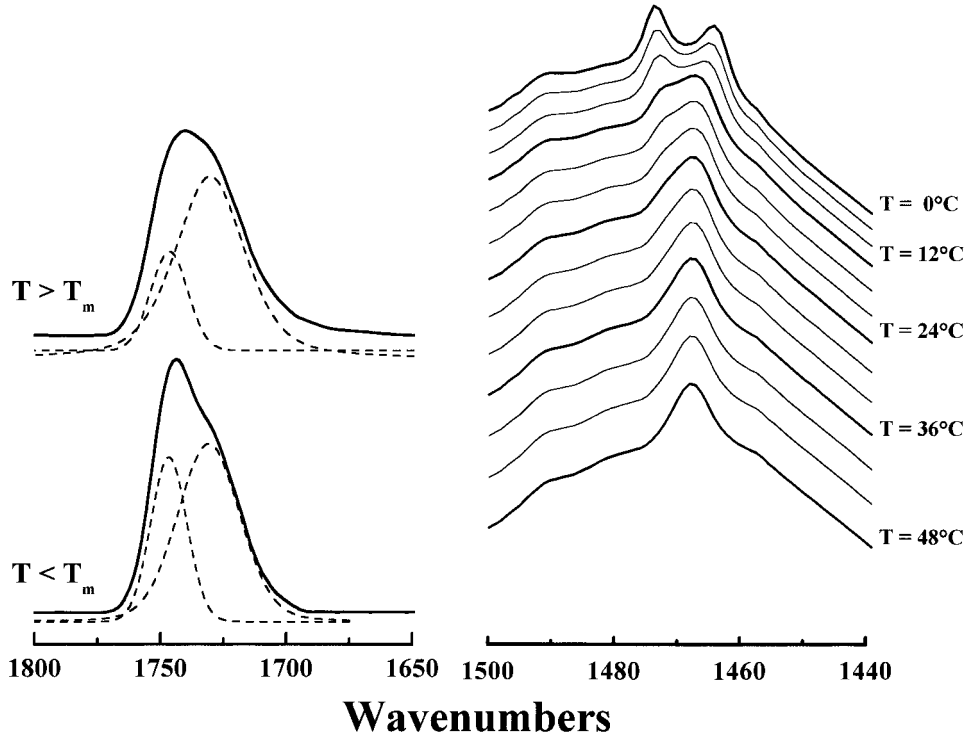

FIGURE 10 Representative FTIR spectra illustrating the changes in the CH_2 scissoring (*right panel*) and C═O stretching (*left panel*) bands of Et-DSPC. The spectra shown in the right panel are presented as a function of temperature and typify the changes in the CH_2 scissoring band coincident with the weak solid phase transition exhibited by the longer-chain compounds. The left panel illustrates the changes in the contours of the C═O stretching band at the gel/liquid-crystalline phase transition. The solid lines illustrate the spectra actually acquired, whereas the dashed lines illustrate our estimates of the properties of the component bands.

can be directly attributed to the packing of the lipid hydrocarbon chains into subcells in which the hydrocarbon chain zigzag planes are perpendicular to each other (see Snyder, 1961, 1979). This spectroscopic feature is generally associated with the arrangement of all-*trans* polymethylene chains in the orthorhombic perpendicular form of subcellular packing (see Lewis and McElhaney, 1996). Upon heating, the factor group splitting of the main CH_2 scissoring bands collapses over a temperature range centered near the midpoint of the solid phase transition, and a single relatively broad absorption band centered near 1468 cm^{-1} is formed (see Fig. 10, *right panel*). Given that the latter frequency is generally associated with hexagonally packed or otherwise rotationally disordered all-*trans* polymethylene chains (see Lewis and McElhaney, 1996), we conclude that the weakly energetic solid-phase transition described above involves a significant reorganization of the packing of the lipid hydrocarbon chains. This conclusion is also supported by the results of our x-ray diffraction (see above). Significant changes in the contours of the main CH_2 scissoring band are not observed upon further heating until the onset of the $L_{\beta I}/L_{\alpha}$ phase transition, whereupon this absorption band broadens without a significant change in its peak frequency. The broadening of this peak is consistent with the increase in hydrocarbon chain mobility that occurs upon the melting of all-*trans* polymethylene chains.

The contours of the C═O stretching absorption band of these lipids also do not change significantly until the onset of the hydrocarbon chain-melting phase transition aside from relatively small increases in overall bandwidth. At temperatures below the T_m, the C═O stretching band consists of an asymmetric absorption envelope with a maximum near 1744 cm^{-1} and, upon melting of the hydrocarbon chains, this band broadens significantly and its peak frequency decreases to values near 1737 cm^{-1}. Further analysis using a combination of Fourier deconvolution and curve-fitting procedures suggests that this observation can be attributed to a phase state-induced change in the intensities of high- and low-frequency components of this absorption band. As illustrated in Fig. 10 (*left panel*), the C═O stretching band of these phospholipids is composed of a relatively broad component centered near 1730–1733 cm^{-1} and a considerably narrower component centered near 1745–1747 cm^{-1}. At the $L_{\beta I}/L_{\alpha}$ phase transition the relative intensity of the lower-frequency component increases significantly, presumably at the expense of the higher-frequency component centered near 1746 cm^{-1}. Given that the high- and low-frequency components of the C═O stretching band envelope of hydrated diacylglycerolipid bilayers are attributable to subpopulations of "free" and hydrogen-bonded ester carbonyl groups, respectively (see Blume et al., 1988; Lewis et al., 1994a), these results suggest that the $L_{\beta I}/L_{\alpha}$ phase transition of these lipid bilayers is accompanied by an increase in the proportion of hydrogen-bonded ester carbonyl groups relative to the free ester carbonyl groups. Moreover, given that interfacial water is the sole source of hydrogen-bonding donor groups present, the $L_{\beta I}/L_{\alpha}$ phase transition must be accompanied by an increase

in the hydration of the polar/apolar interfacial regions of these bilayers. Finally, we note that the weakly energetic phase transition that occurs at ~40°C below the T_m is not accompanied by any discernible change in the contours of the C═O stretching band. The latter observation clearly indicates that the weakly energetic solid phase event does not involve any significant changes in the conformation, hydration, and general organization of the ester carbonyl groups at the polar/apolar interfaces of these phospholipid bilayers.

DISCUSSION

Our results indicate that aspects of the thermotropic phase behavior, structure, and organization of bilayers composed of cationic Et-PCs differ significantly from those of the corresponding PC bilayers. The transition temperatures and transition enthalpy values determined by us and others (MacDonald et al., 1999a) are higher than those of the corresponding PCs, suggesting that these cationic lipids form more stable gel phases than do the corresponding PCs. Most probably, this can be attributed to the fact that these cationic PC derivatives form hydrocarbon chain-interdigitated gel phases at temperatures below the T_m. Evidence supporting this conclusion was obtained from the small-angle x-ray diffraction data, which show that the *d* spacings of aqueous Et-DMPC, Et-DPPC, and Et-DSPC dispersions all increase significantly at the gel/liquid-crystalline phase transition, and was confirmed by the one-dimensional electron density profiles calculated from the same data. Comparable behavior has been observed with 1,3-DPPC, 1,2-dihexadecyl PC, and 1-*O*-palmitoyl, 2-*O*-(16-fluoropalmitoyl) PC, lipids which all form hydrocarbon chain interdigitated phases (Serrallach et al., 1983; Ruocco et al., 1985; Kim et al., 1987; Laggner et al., 1987; Hirsh et al., 1998). Similar behavior is also exhibited by PC and phosphatidylglycerol bilayers under conditions where gel-state hydrocarbon chain interdigitation is induced by the inclusion of short-chain alkanols such as ethanol (Simon and McIntosh, 1984) or by dispersion in low ionic strength Tris-buffered media (Wilkinson et al., 1987).

The propensity of these cationic lipids to form $L_{\beta I}$ phases raises some fundamental questions about the molecular basis of this aspect of their behavior. It has been determined that the conversion from a noninterdigitated to a fully interdigitated all-*trans* polymethylene chain packing format can result in a free energy gain of some 130 cal/mol per CH_2 group (Simon and McIntosh, 1984). However, with all amphipathic lipid bilayers, the transition from a noninterdigitated to a fully interdigitated state incurs a significant energetic cost due to the exposure of the hydrophobic ends of the hydrocarbon chains to the aqueous phase and/or to the polar moieties of the phospholipid headgroup and glycerol backbone regions. Also, because interdigitation increases the mean separation of the polar headgroups, it could incur an additional energy cost attributable to decreased lateral attractive interactions between the polar headgroups or, depending upon the chemical structure of the polar headgroup, interdigitation could be facilitated by the relief of stress arising from charged-group repulsion and/or steric crowding of the polar headgroups. It therefore follows that increases in hydrocarbon chain length, modifications of the lipid headgroup, and/or changes in the composition of the aqueous phase which diminish the energetic cost of their interaction with hydrophobic groups, increases in headgroup steric bulk, and increases in the net charge of the polar headgroup should all favor the formation of a hydrocarbon chain-interdigitated gel state in preference to a noninterdigitated phase. With these cationic PC derivatives, the manifestation of the above factors is probably directly or indirectly related to the presence of the ethyl group esterified to the phosphate moiety. This is because esterification of phosphate moiety of a PC molecule increases the steric bulk of its polar headgroup and converts the zwitterionic lipid into a positively charged species. These changes should destabilize the noninterdigitated gel phase because of a combination of increased stress attributable to steric crowding and charge repulsion. Also, with the esterification of the PC phosphate moiety, there is a decrease in its overall polarity and, through its interactions with the bilayer polar/apolar interface, there may be a decrease in interfacial polarity as well. Moreover, the headgroup ethyl moiety may interact directly with the bilayer polar/apolar interface and lower the overall polarity of that region of the bilayer. A decrease in the polarity of the bilayer polar/apolar interface, together with the decreased polarity of the neighboring phosphate moiety, should facilitate hydrocarbon chain interdigitation by reducing the energetic cost of locating the hydrophobic ends of the lipid chains amid polar moieties in the headgroup region and/or at the bilayer polar/apolar interface. In support of the above suggestions, our infrared spectroscopic data provide evidence that the polar/apolar interfaces of these cationic PC derivatives are less polar than those of the corresponding PC bilayers. Also, the suggested mechanism of whereby hydrocarbon chain interdigitation could be facilitated by the penetration of the headgroup ethyl groups into the bilayer polar/apolar interface is conceptually compatible to the mechanism whereby ethanol is believed to induce the interdigitation of PC hydrocarbon chains (see Simon and McIntosh, 1984).

Hydrocarbon chain interdigitation may also provide a rationale for other aspects of the thermotropic phase behavior of these cationic PC derivatives. For example, these lipids exhibit a single, highly cooperative hydrocarbon chain-melting endotherm upon heating and, upon cooling from temperatures above T_m, they exhibit two cooling exothermic transitions which have both been identified as transitions from liquid-crystalline to gel phases. A similar pattern of thermotropic phase behavior has been observed in studies of mixed-chain PCs that form interdigitated gel

phases (see Lewis et al., 1994b). Subsequently it was determined that at liquid-crystalline temperatures, multilamellar dispersions of those mixed-chain PCs contain two morphologically distinct populations of lipids and the two cooling exotherms were assigned to the differential freezing of lipid chains in the two populations (Mason et al., 1995). Recent studies of aqueous dispersions of P-O-ethyl dioleoyl phosphatidylcholine demonstrate that multilamellar dispersions of this lipid also contain two populations of differently sized lamellar particles (see MacDonald et al., 1999a). We therefore suggest that the anomalous cooling behavior exhibited by these cationic lipids may also be attributable to the differential freezing of lipids in these two populations. The reasons why interdigitated lipid bilayers may be prone to this type of thermotropic phase behavior are yet to be determined.

Hydrocarbon chain interdigitation may also constitute the basis of the weakly energetic solid-phase transition exhibited by the longer-chain homologs. Our data show that this thermotropic event is not correlated with any discernible change in the rates or amplitude of phosphate reorientation nor is it accompanied by any significant change in the hydration and/or conformation of moieties in the bilayer polar/apolar interface. Also, both x-ray diffraction and FTIR spectroscopic data indicate that this thermotropic event involves a reversible interconversion between orthorhombically packed and hexagonally packed hydrocarbon chain subcells. This thermotropic change is exclusively a hydrocarbon chain packing event and as such it can occur in double-chained amphiphiles such as glycerolipid bilayers only when lateral interactions between lipid polar headgroups and between moieties in the bilayer polar/apolar interface are relatively weak. Such requirements can be fulfilled in fully interdigitated glycerolipid bilayers. A similar type of thermotropic event has been observed in the interdigitated gel phase of dihexadecyl phosphatidylcholine (Laggner et al., 1987; Lewis et al., 1996).

The shapes of the ^{31}P-NMR powder patterns exhibited by the $L_{\beta I}$ phases of these cationic PC bilayers are not typical of the axially symmetric ^{31}P-NMR spectra exhibited by the L_{β} phases of the corresponding PCs or by the gel phases of other phospholipids in which hydrocarbon chain interdigitation is known to occur (see Ruocco et al., 1985; Xu et al., 1987; Peng and Jonas, 1992). However, it is unlikely that our results can be attributed to markedly different rates of phosphate headgroup reorientation because the gel-phase basal linewidths of the ^{31}P-NMR powder patterns exhibited by these lipids are comparable to those of the gel phases of other phospholipids. It is thus more likely that the range of phosphate headgroup reorientational motion in the gel phase of these cationic lipid bilayers differs significantly from those of most other phospholipids because of motional constraints that are not normally encountered in the latter. Currently, it is not clear why the reorientation motions of phosphate headgroups in the gel phases of these cationic lipids should be markedly different from those occurring in the gel phases of most other phospholipid bilayers, nor is it clear what the nature of these motional constraints may be. However, we can suggest the following possibilities. First, because these polar headgroups are positively charged, their motions may be constrained by the necessity of minimizing close approach contacts between positively charged quaternary ammonium groups and, unlike the zwitterionic PCs, such tendencies would not be balanced by any tendency to maximize contacts between the positively charged quaternary ammonium groups and neighboring negatively charged phosphate groups. Second, it is also possible that the reorientational motions of the ethyl phosphorylcholine headgroups are further constrained to facilitate contacts between the headgroup ethyl groups and moieties in the bilayer polar/apolar interface (see above). We therefore suggest that the combined effects of these two factors could have resulted in a preferred conformation of the ethyl phosphoryl choline moiety that differs significantly from that of the phosphate headgroups in the gel phases of most other phospholipid bilayers.

Our studies of Et-DLPC reveal a number of other interesting features. In particular, although aqueous dispersions of this lipid exhibit ^{31}P-NMR data consistent with the formation of slowly tumbling large lamellar structures, the x-ray diffraction data indicate that Et-DLPC does not form multilamellar dispersions when dispersed in aqueous media under our conditions. These observations suggest the formation of uncorrelated lipid lamellae, the result of excessive swelling of the interlamellar spaces owing to charge repulsion between the positively charged lipid surfaces. However, comparable behavior was not observed with the longer-chain homologs, although continuous and excessive swelling of the interlamellar spaces often occurs when charged lamellar-forming amphiphiles are dispersed in low ionic-strength aqueous media (see Hauser, 1984; Koynova et al., 1993). The possibility of a chain length-dependent component to this type of behavior is also consistent with the results of recent x-ray diffraction studies, which demonstrate that whereas aqueous dispersions of the cationic amphiphile di-*O*-myristoyl-3-*N*,*N*,*N*-trimethylaminopropane forms uncorrelated lamellae in the fluid phase (Lewis et al., 2000), the longer chain di-*O*-oleoyl derivative forms large multilamellar structures under comparable conditions (Koltover et al., 1999). It should also be noted that a chain-length-dependent change in aggregation state also occurs with the n-saturated 1,2-diacyl PCs for which dioctanoylPC ($n = 8$) forms micelles, dinonaoylPC ($n = 9$) forms unilamellar vesicles, and those PCs with chain-lengths of 10 or more carbon atoms form multilamellar vesicles (see Racey et al., 1989).

Our studies also show that unlike the longer-chain homologs, Et-DLPC exhibits a reversible weakly energetic thermotropic transition some 8°C above its gel/liquid-crystalline phase transition. As noted above this transition is not

a lamellar/nonlamellar phase transition and our x-ray diffraction results suggest that it may involve a cooperative change in the conformation of the headgroup phosphate moiety. It is interesting to note, however, that this thermotropic event occurs at temperatures close to 4°C, where water approaches its maximum density. It is therefore possible that the cooperative change in phosphate headgroup conformation may be linked to, or triggered by, the changing patterns of hydrogen-bonding interactions that occur when water approaches its maximal density.

Finally, these experimental measurements enable the construction of a fairly detailed picture of the structure and organization of bilayers composed of these cationic PC derivatives and of the nature of the thermotropic transitions exhibited by them. At low temperatures the behavior of these lipids is dominated by the packing requirements of the hydrocarbon chains and, under such conditions, a fully interdigitated gel phase is formed in which the hydrocarbon chains assemble into a near-optimal form of orthorhombic perpendicular packing. Upon heating, thermally induced increases in the rates and amplitudes of hydrocarbon chain reorientational fluctuations eventually cause the breakdown of this form of subcellular packing and the hydrocarbon chains convert to a hexagonal packing format in which the chains are essentially orientationally disordered. Further heating results in a progressive weakening of the lateral interactions between the hydrocarbon chains culminating with the hydrocarbon chain-melting phase transition. The progressive decline of these lateral packing interactions make the interdigitated state progressively less stable with respect to a noninterdigitated packing format and, at the hydrocarbon chain-melting phase transition, the system reverts to a noninterdigitated format when the energy gained from the lateral interactions of interdigitated hydrocarbon chains no longer meets the energetic cost of locating the hydrophobic ends of the lipid chains amid polar moieties. The conversion to the liquid-crystalline state is also accompanied by an increased penetration of water into the bilayer polar/apolar interfacial region and by an increase in the rates of phosphate headgroup reorientation. However, because of the esterification of the phosphate, the negatively charged polar group normally located in proximity to the bilayer polar/apolar interface is replaced by a bulkier less polar and uncharged polar group. The net effect of these changes is that polar/apolar interfaces and the proximal headgroup regions of these cationic lipid bilayers are less polar than those of naturally occurring phospholipid bilayers, and this factor limits the penetration of water into these critical regions. Aside from the positively charged surface, this latter property markedly distinguishes the liquid-crystalline phases of bilayers composed of these cationic PC derivatives from those composed of the corresponding zwitterionic PCs, and may be relevant to proposed technological applications of this class of cationic lipid bilayers.

This work was supported by operating and major equipment grants from the Canadian Institutes of Health Research (to R.N.M.), by major equipment grants from the Alberta Heritage Foundation for Medical Research (to R.N.M.), and by a National Grant of the Austrian Ministry of Science and Transportation (to K.L.), as well as by the Österreichische Nationalbank (Jubiläumsfondsprojekt No. 7190, to K.L.). Also, we are indebted to Dr. Brian D. Sykes of the Department of Biochemistry at the University of Alberta for the generous availability of time on the NMR spectrometer.

REFERENCES

Barber, K., R. R. Mala, M. P. Lambert, R. Qui, R. C. MacDonald, and W. L. Klein. 1996. Delivery of membrane-impermeant fluorescent probes into living neural cell populations by lipotransfer. *Neurosci. Lett.* 207:17–20.

Bennett, C. F., M. Y. Chiang, H. Chan, J. E. Shoemaker, and C. K. Mirabelli. 1992. Cationic lipids enhance cellular uptake and activity of phosphorothioate antisense oligonucleotides. *Mol. Pharmacol.* 41: 1023–1033.

Blume, A., W. Hübner, and G. Messner. 1988. Fourier transform infrared spectroscopy of $^{13}C{=}O$ labeled phospholipids. Hydrogen bonding to carbonyl groups. *Biochemistry.* 27:8239–8249.

Bouwstra, J. A., G. S. Gooris, W. Bras, and H. Talsma. 1993. Small angle x-ray scattering: possibilities and limitations in characterization of vesicles. *Chem. Phys. Lipids.* 64:83–98.

Braganza, L. F., and D. L. Worcester. 1986. Hydrostatic pressure induces hydrocarbon chain interdigitation in single-component phospholipid bilayers. *Biochemistry.* 25:2591–2596.

Campbell, R. F., F. E. Meirovitch, and J. H. Freed. 1979. Slow motional line NMR lineshapes for very anisotropic rotational diffusion phosphorous-31 NMR of phospholipids. *J. Phys. Chem.* 83:525–533.

Debs, R. J., L. P. Freedman, S. Edmunds, K. L. Gaensler, N. Duzgunes, and K. R. Yamamoto. 1990. Regulation of gene expression in vivo by liposome-mediated delivery of a purified transcription factor. *J. Biol. Chem.* 265:10189–10192.

Felger, P. L. 1995. The evolving role of the liposome in gene delivery. *J. Liposome Res.* 5:725–734.

Furuike, S., V. G. Levadny, S. J. Li, and M. Yamazaki. 1999. Low pH induces an interdigitated gel to bilayer gel phase transition in dihexadecyl phosphatidylcholine membrane. *Biophys. J.* 77:2015–2023.

Glatter, O. 1977. A new method for the evaluation of small-angle scattering data. *J. Appl. Crystallogr.* 10:415–421.

Glatter, O. 1982a. Data treatment. *In* Small Angle X-ray Scattering. O. Glatter and O. Kratky, editors. Academic Press Inc., London. 119–166.

Glatter, O. 1982b. Interpretation. *In* Small Angle X-ray Scattering. O. Glatter and O. Kratky, editors. Academic Press Inc., London. 167–196.

Gorman, C. M., M. Aikawa, B. Fox, E. Fox, C. Lapuz, B. Michaud, H. Nguyen, E. Roche, T. Sawa, and J. P. Wiener-Kronish. 1997. Efficient in vivo delivery of DNA to pulmonary cells using the novel lipid EDMPC. *Gene Therapy.* 4:983–992.

Gregoriadis, G. 1995. Engineering liposomes for drug delivery: progress and problems. *Trends Biotechnol.* 13:527–537.

Hauser, H. 1984. Some aspects of the phase behavior of charged lipids. *Biochim. Biophys. Acta.* 772:37–50.

Hirsh, D. J., N. Lazaro, L. R. Wright, J. M. Boggs, T. J. McIntosh, J. Schaefer, and J. Blazyk. 1998. A new monofluorinated phosphatidylcholine forms interdigitated bilayers. *Biophys. J.* 75:1858–1868.

Huang, L., H. Farhood, N. Serbina, A. G. Teepe, and J. Barsoum. 1995. Endosomolytic activity of cationic liposomes enhances the delivery of human immunodeficiency virus-1 trans-activator protein (TAT) to mammalian cells. *Biochem. Biophys. Res. Commun.* 217:761–767.

Huang, C., and T. J. McIntosh. 1997. Probing the ethanol-induced chain interdigitations in gel-state bilayers of mixed-chain phosphatidylcholines. *Biophys. J.* 72:2702–2709.

Hui, S. W., J. T. Mason, and C. Huang. 1984. Acyl chain interdigitation in saturated mixed-chain phosphatidylcholine bilayer dispersions. *Biochemistry.* 23:5570–5577.

Kim, J. T., J. Mattai, and G. G. Shipley. 1987. Gel phase polymorphism in ether-linked dihexadecyl phosphatidylcholine bilayers. *Biochemistry.* 26:6592–6598.

Koltover, I., T. Salditt, and C. R. Safinya. 1999. Phase diagram, stability and overcharging of lamellar cationic lipid-DNA self assembled complexes. *Biophys. J.* 77:915–924.

Konstantinova, I. D., and G. A. Serebrinnikova. 1996. Positively charged lipids: structure and application. *Uspejhi Khimi.* 65:581–598.

Koynova, R. D., B. G. Tenchov, H. Kuttenreich, and H.-J. Hinz. 1993. Structure and phase behavior of a charged glycolipid (1, 2-O-dialkyl-3-O-β-d-glucuronosyl-sn-glycerol). *Biochemistry.* 32:12437–12445.

Kriechbaum, M., and P. Laggner. 1996. States of phase transition in biological structures. *Prog. Surface Sci.* 51:233–261.

Laggner, P. 1994. X-ray diffraction on biomembranes with emphasis on lipid moiety. *In* Subcellular Biochemistry, Vol. 23. Physico-Chemical Methods in the Study of Biomembranes. H. J. Hilderson and G. B. Ralston, editors. Plenum Press, New York. 451–491.

Laggner, P., K. Lohner, G. Degovics, K. Müller, and A. Schuster. 1987. Structure and thermodynamics of the dihexadecyl phosphatidylcholine-water system. *Chem. Phys. Lipids.* 44:31–60.

Lewis, R. N. A. H., and R. N. McElhaney. 1996. Fourier transform infrared spectroscopy in the study of hydrated lipids and lipid bilayer membranes. *In* Infrared Spectroscopy of Biomolecules. H. H. Mantsch and D. Chapman, editors. Wiley-Liss, New York. 159–202.

Lewis, R. N. A. H., and R. N. McElhaney. 2000. Membrane surface charge markedly attenuates the nonlamellar phase-forming propensities of lipid bilayer membranes. Calorimetric and ^{31}P-nuclear magnetic resonance studies of mixtures of cationic, anionic and zwitterionic lipids. *Biophys. J.* 79:1455–1464.

Lewis, R. N. A. H., R. N. McElhaney, F. Österberg, and S. M. Gruner. 1994b. Enigmatic thermotropic phase behavior of highly asymmetric mixed-chain phosphatidylcholines which form mixed-interdigitated gel phases. *Biophys. J.* 66:207–216.

Lewis, R. N. A. H., R. N. McElhaney, W. Pohle, and H. H. Mantsch. 1994a. The components of the carbonyl stretching band in the infrared spectra of hydrated 1,2-diacylglycerolipid bilayers: a reevaluation. *Biophys. J.* 67:2367–2375.

Lewis, R. N. A. H., W. Pohle, and R. N. McElhaney. 1996. The interfacial structure of phospholipid bilayers: differential scanning calorimetric and Fourier transform infrared spectroscopic studies of 1,2-dipalmitoyl-*sn*-glycero-3-phosphorylcholine and its dialkyl and acyl-alkyl analogs. *Biophys. J.* 70:2736–2746.

Lewis, R. N. A. H., E. J. Prenner, L. H. Kondejewski, C. R. Flach, R. Mendelsohn, R. S. Hodges, and R. N. McElhaney. 1999. Fourier transform infrared spectroscopic studies of the interaction of the antimicrobial peptide Gramicidin S with lipid micelles and with lipid monolayer and bilayer membranes. *Biochemistry.* 38:15193–15203.

Lewis, R. N. A. H., B. D. Sykes, and R. N. McElhaney. 1988. The thermotropic phase behavior of model membranes composed of phosphatidylcholines containing *cis*-monounsaturated acyl chain homologues of oleic acid: differential scanning calorimetric and ^{31}P-NMR spectroscopic studies. *Biochemistry.* 27:880–887.

Lewis, R. N. A. H., S. Tristram-Nagle, J. F. Nagle, and R. N. McElhaney, R. N. 2000. Studies of the thermotropic phase behavior of cationic lipid membranes. Calorimetric, spectroscopic and x-ray diffraction studies of lipid bilayers composed of 1,2-di-O-myristoyl-3-N,N,N-trimethylaminopropane (DM-TAP). *Biochim. Biophys. Acta.* (in press).

MacDonald, R. C., G. W. Ashley, M. M. Shida, V. A. Rakhmanova, Y. S. Tarahovsky, D. P. Pantazatos, M. T. Kennedy, E. V. Pozharski, K. A. Baker, R. D. Jones, H. Rosenzweig, K. L. Choi, R. Qiu, and T. J. McIntosh. 1999a. Physical and biological properties of cationic triesters of phosphatidylcholine. *Biophys. J.* 77:2612–2629.

MacDonald, R. C., V. A. Rakhmanova, K. L. Choi, H. S. Rosenzweig, and M. K. Lahiri. 1999b. O-Ethyl phosphatidylcholine: a metabolizable cationic phospholipid which is a serum compatible DNA transfection agent. *J. Pharm. Sci.* 88:896–904.

Mantsch, H. H., C. Madec, R. N. A. H. Lewis, and R. N. McElhaney. 1985. Thermotropic phase behavior of model membranes composed of phosphatidylcholines containing isobranched fatty acids. 2. Infrared and ^{31}P-NMR spectroscopic studies. *Biochemistry.* 24:2440–2446.

Mason, J. T., R. E. Cunningham, and T. J. O'Leary. 1995. Lamellar-phase polymorphism in interdigitated bilayer assemblies. *Biochim. Biophys. Acta.* 1236:65–72.

Matsumura, J. S., R. Kim, V. P. Shively, R. C. MacDonald, and W. H. Pearce. 1999. Characterization of vascular gene transfer using a novel cationic lipid. *J. Surgical Res.* 85:339–345.

Maulik, P. R., M. J. Ruocco, and G. G. Shipley. 1990. Hydrocarbon chain packing modes in lipids: effect of altered subcell dimensions and chain rotation. *Chem. Phys. Lipids.* 56:123–133.

McDonald, R. J., H. D. Liggitt, L. Roche, H. T. Nguyen, R. Pearlman, O. G. Raabe, L. B. Bussey, and C. M. Gorman. 1998. Aerosol delivery of lipid:DNA complexes to lungs of rhesus monkeys. *Pharm. Res.* 15:671–679.

McIntosh, T. J., R. V. McDaniel, and S. A. Simon. 1983. Induction of an interdigitated gel phase in fully hydrated lecithin bilayers. *Biochim. Biophys. Acta.* 731:109–114.

Morgan, R. A., and W. F. Anderson. 1993. Human gene therapy. *Annu. Rev. Biochem.* 62:191–217.

Nambi, P., E. S. Rowe, and T. J. McIntosh. 1988. Studies of the ethanol-induced interdigitated gel phase in phosphatidylcholines using the fluorophore 1,6-diphenyl-1,3,5-hexatriene. *Biochemistry.* 27:9175–9182.

Pantazatos, D. P., and R. C. MacDonald. 1999. Directly observed membrane fusion between oppositely charged phospholipid bilayers. *J. Membr. Biol.* 170:27–38.

Peng, X., and J. Jonas. 1992. High-pressure ^{31}P NMR study of dipalmitoylphosphatidylcholine bilayers. *Biochemistry.* 31:6383–6390.

Racey, T. J., M. A. Singer, L. Finegold, and P. Rochon. 1989. The influence of fatty acyl chain length and head group on the size of multilamellar vesicles. *Chem. Phys. Lipids.* 49:271–288.

Ranck, J. L., T. Keira, and V. Luzzati. 1977. A novel packing of the hydrocarbon chains in lipids. *Biochim. Biophys. Acta.* 488:432–441.

Ruocco, M. J., D. J. Siminovitch, and R. G. Griffin. 1985. Comparative study of the gel phases of ether- and ester-linked phosphatidylcholines. *Biochemistry.* 24:2406–2411.

Seelig, J. 1978. ^{31}P nuclear magnetic resonance and the headgroup structure of phospholipid membranes. *Biochim. Biophys. Acta.* 515:105–140.

Serrallach, E. N., R. Dijkman, G. H. de Haas, and G. G. Shipley. 1983. Structure and thermotropic properties of 1,3-dipalmitoyl-glycero-2-phosphocholine. *J. Mol. Biol.* 170:155–174.

Simon. S. A., and T. J. McIntosh. 1984. Interdigitated hydrocarbon chain packing causes the biphasic transition behavior in lipid/alcohol suspensions. *Biochim. Biophys. Acta.* 773:169–172.

Snyder, R. G. 1961. Vibrational spectra of crystalline n-paraffins II. Intermolecular effects. *J. Mol. Spectrosc.* 7:116–144.

Snyder, R. G. 1979. Vibrational correlation splitting and chain packing for the crystalline alkanes. *J. Chem. Phys.* 71:3229–3235.

Tardieu, A., V. Luzzatti, and F. C. Reman. 1973. Structure and polymorphism of the hydrocarbon chains of lipids: a study of lecithin-water phases. *J. Mol. Biol.* 75:711–733.

Wiener, M. C., R. M. Suter, and J. F. Nagle. 1989. Structure of the fully hydrated gel phase of dipalmitoylphosphatidylcholine. *Biophys. J.* 55: 315–325.

Wilkinson, D. A., D. A. Tirrell, A. B. Turek, and T. J. McIntosh. 1987. Tris buffer causes acyl chain interdigitation in phosphatidylglycerol. *Biochim. Biophys. Acta.* 905:447–453.

Xu, H., F. A. Stephenson, and C. H. Huang. 1987. Binary mixtures of asymmetric phosphatidyl-cholines with one acyl chain twice as long as the other. *Biochemistry.* 26:5448–5453.

Zhou, F., and L. Huang. 1994. Liposome-mediated cytoplasmic delivery of proteins: an effective means of accessing the MHC class I-restricted antigen presentation pathway. *Immunomethods.* 4:229–235.